

Preliminary Proton and Helium Spectra from the CREAM-III Flight

Y. S. Yoon^{*†}, H. S. Ahn^{*}, T. Anderson[‡], L. Barbier[§], A. Barrau[¶], R. Bazer-Bach^{||}, J. J. Beatty^{**},
P. Bhojar^{*}, T. J. Brandt^{**}, M. Buénerd[¶], N. B. Conklin[‡], S. Coutu[‡], L. Derome[¶],
M. A. DuVernois^{††}, O. Ganel^{*}, M. Geske[‡], J. H. Han^{*}, J. A. Jeon^{‡‡}, K. C. Kim^{*}, M. H. Lee^{*},
J. T. Link^{§^x}, A. Malinin^{*}, M. Mangin-Brinet[¶], A. Menchaca-Rocha^{xi}, J. W. Mitchell[§],
S. I. Mognet[‡], G. Na^{‡‡}, S. Nam^{‡‡}, S. Nutter^{xii}, I. H. Park^{‡‡}, N. H. Park^{‡‡}, A. Putze[¶],
J.N. Périé^{||}, Y. Sallaz-Damaz[¶], E. S. Seo^{*†}, P. Walpole^{*}, J. Wu^{*}, J. Yang^{‡‡}, J. H. Yoo^{*}

^{*}*Institute of Physical Science and Technology, University of Maryland, College Park, Maryland, 20742, USA*

[†]*Department of Physics, University of Maryland, College Park, Maryland, 20742, USA*

[‡]*Department of Physics, Penn State University, University Park, PA 16802, USA*

[§]*Astrophysics Space Division, NASA Goddard Space Flight Center, Greenbelt, MD 20771, USA*

[¶]*Laboratoire de Physique Subatomique et de Cosmologie, Grenoble, France*

^{||}*Center d'Etude Spatiale des Rayonnements, UFR PCA-CNRS-UPR 8002, Toulouse, France*

^{**}*Department of Physics, Ohio State University, Columbus, OH 43210, USA*

^{††}*Department of Physics, University of Hawaii, Honolulu, Hawaii 96822, USA*

^{‡‡}*Department of Physics, Ewha Womans University, Seoul 120-750, Republic of Korea*

^x*CRESST/USRA, Columbia, MD 21044, USA*

^{xi}*Instituto de Fisica, Universidad Nacional Autonoma de Mexico, Mexico*

^{xii}*Department of Physics, Northern Kentucky University, Highland Heights, KY 41099, USA*

Abstract. The balloon-borne Cosmic Ray Energetics And Mass (CREAM) instrument measures the composition and energy spectra of primary cosmic rays. CREAM has flown four times over Antarctica. The CREAM-III payload flew for 29 days during the 2007-2008 Antarctic season. The electronics of the calorimeter were improved from a 12-bit to a 16-bit readout, with reduced pedestal noise level, and removal of a temperature dependence in the pedestal values. With these improvements, the flight accumulated significantly more data at lower energies than the two previous flights. Energy measurements of incident particles were made using the calorimeter flight data, taking into account a calorimeter calibration performed at CERN (European Organization for Nuclear Research). The energy spectra were corrected for event selection efficiency, trigger efficiency, and reconstruction efficiency, as well as backgrounds determined with Monte Carlo simulations. Preliminary results for the proton and helium fluxes and proton to helium ratio obtained from the flight data are presented.

Keywords: CREAM; energy spectra; protons and helium nuclei

I. INTRODUCTION

Energy spectra of primary cosmic rays are known with good precision up to energies around 10^{12} eV. Above this energy, the composition of cosmic rays and their energy spectra are not well known although there have been some measurements ([1], [2]). For example,

Asakimori, *et al.* (1998) reported a difference in the spectral indices for protons and helium, but Apanasenko, *et al.* (1999) did not see such a difference. More accurate measurements above a few TeV are therefore needed.

CREAM is a balloon-borne experiment to measure elemental spectra of cosmic-ray nuclei in the energy range $\sim 10^{11} - 10^{15}$ eV from protons to iron [3]. The goal is to extend direct cosmic-ray composition measurements to the highest energies practical with balloon flights. The CREAM instrument has flown four times over Antarctica since 2004. The CREAM-III payload was launched on December 19, 2007 and the flight was terminated on January 17, 2008 after ~ 29 days of flight.

II. CREAM-III INSTRUMENT AND FLIGHT

The CREAM-III instrument consisted of a tungsten/scintillating fiber calorimeter, a dual layer Silicon Charge Detector (SCD), a Cherenkov Camera (CherCam), a Cherenkov Detector, and a Timing Charge Detector (TCD). The calorimeter measures the energy of incident nuclei that interact in graphite targets located directly above it, while the SCD, CherCam, and TCD provide charge identification of incident particles. More details about the detectors can be found elsewhere ([5], [6], [7], [8]).

The calorimeter is comprised of a stack of 20 tungsten layers with an overall 20 radiation length (X_0) depth and 20 layers of scintillating fibers. The fibers are arranged into fifty 1 cm wide ribbons per layer, each

read out independently. Clear fibers connected to each ribbon were divided into low, middle and high ranges, to increase the dynamic range.

Two separate layers of the SCD provide independent charge measurements with a resolution of $\sim 0.2 e$. Both of top and bottom SCD layers have 2688 pixels; each pixel has 2.12 cm^2 area. This paper describes preliminary analysis from the calorimeter and top SCD.

Throughout the CREAM-III flight, the calorimeter performed stably without any high-voltage issues. The live-time fraction during data collection was about 99%.

The electronics of the calorimeter were improved from previous CREAM flights [9]. An improved Application-Specific Integrated Circuit (ASIC) board design reduced the front-end electronics noise level. The 12 bit Analog-to-Digital Converter (ADC) chip was replaced with a 16 bit chip to increase the dynamic range. The pedestal drift with temperature was removed [10]. The reduced noise level allowed the trigger thresholds to be lowered to about 15 MeV, whereas it was about 50 MeV for the two previous flights. Also, Sparsification threshold value (STV) in each channel, which suppress the pedestal, was lowered to about 2σ of the pedestal.

III. ANALYSIS

A. Calibration

The CREAM-III calorimeter and SCD were calibrated at CERN using 150 GeV electrons in 2006 [9], [11]. Conversion factors from the ADC signal to MeV were obtained from the ratio of measured ADC values to the deposited energy in each ribbon according to a Monte Carlo (MC) simulation based on GEANT/FLUKA 3.21 [12], [13].

The linearity of the output signal at different high-voltages for a hybrid photo diode was confirmed, and the ratio of deposited energy at 10.5 kV to deposited energy at 6 kV was found to be 2.0. This ratio was used for gain correction due to the high-voltage difference between the calibration test and the flight.

Channels connected to the low ranges were calibrated with 150 GeV electrons during the beam test [14]. Channels connected to middle and high ranges were calibrated with a combination of the ratios of number of fibers in each range and the low range calibration constants. Another method was to use the ratios of signal outputs from the low and middle ranges for middle range calibration and ratios of signal outputs from middle and high ranges for high range calibration in each ribbon from the flight data. In this analysis, the latter was used for middle range calibration.

B. Event Selection

The calorimeter trigger selects high energy shower events in an unbiased manner by requiring 6 consecutive layers, each with at least one ribbon recording more

than trigger thresholds, 15 MeV. 99.8% of the CREAM-III events with a calorimeter trigger flag satisfied the calorimeter trigger condition.

The shower axes were reconstructed in both the X-Z and Y-Z planes for each event. The trajectory in the calorimeter was reconstructed from the ribbon with the highest energy deposit and neighboring ribbons on both sides with hits in at least three layers. The reconstructed trajectory must traverse the top SCD active area and at the bottom of the calorimeter active area.

Events with a late shower or late interaction position could cause an underestimation of the deposited energy or a misidentification of the charge due to a lack of reconstruction information or a poor reconstruction. Therefore, only events with an interaction in the carbon target or in the top layers of the calorimeter are defined as good events. Events with interactions started above top 6 layers in the calorimeter were selected.

C. Charge Determination

The charge identification for this analysis uses the top SCD in order to have conditions similar to the CREAM-I analysis. The dual SCD setup provides two independent charge measurements, so a pure sample of events can be selected by requiring consistency of the charge measurement in both layers. This also improves statistics, since the signal in dead or noisy pixels on one SCD layer could be replaced with the signal from the other SCD layer. An analysis using full CREAM-III detector capabilities is planned for the future.

A 7×7 pixel area centered on the extrapolated position in the top SCD from the reconstructed trajectory is scanned for the highest pixel signal. The measured charge histogram is shown in Fig. 1. The signal in that pixel is then corrected for the reconstructed incidence angle. The number of protons and helium nuclei is determined by calculating the areas under Landau fits for the two peaks in each energy bin. Charge resolutions for both protons and helium are about $0.2 e$.

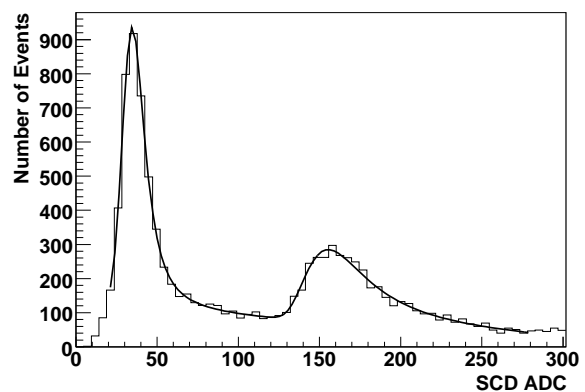


Fig. 1. Top SCD signal distributions. The peak at 40 ADC unit is due to protons and the peak at 160 ADC unit is from helium nuclei. Charge resolution for both protons and helium is $0.2 e$.

D. Energy Measurement

Entries in deposited energy bins are deconvolved to incident energy bins using matrix relations. The counts $N_{inc,i}$ in the incident energy bin i is estimated from the measured counts $N_{dep,i}$ in deposited energy bin j by the relation

$$N_{inc,i} = \sum_j P_{i,j} \cdot N_{dep,j}, \quad (1)$$

where the matrix element $P_{i,j}$ is the probability that the events in the deposited energy bin j are from incident energy bin i ([15]). The matrix elements $P_{i,j}$ are estimated with a MC simulation.

MC simulations to model the CREAM-III detector configuration are in progress. Existing MC simulation events sets generated with the CREAM-I detector configuration were used to calculate $P_{i,j}$ by using the CREAM-III calorimeter flight conditions such as STV and electronics noise smearing. Uncertainties due to different or more detector material above the SCD causing higher background, is not expected to cause a significant difference. Analysis with more MC simulation events with the proper detector configuration will be done in the future.

E. Absolute Flux

The differential flux (F) at the top of atmosphere in each energy bin with size ΔE is given by

$$F = \frac{N_{inc}}{\Delta E \cdot GF \cdot \varepsilon \cdot T \cdot \eta}, \quad (2)$$

where N_{inc} is the number of events in the energy bin, GF is the geometry factor, ε is the efficiency, δ is the background, T is the live time, and η is the correction due to atmospheric attenuation.

The geometry factor was calculated with MC simulation information by requiring that the reconstructed trajectory traverse the top SCD active area and the bottom of the calorimeter. The geometry factor for protons and helium is $0.41 \text{ m}^2 \text{ sr}$.

The efficiency ε can be expressed as the product of event selection efficiency, trigger efficiency, and reconstruction efficiency. Event selection efficiencies for protons and helium nuclei are 89% and 90%, respectively; trigger efficiencies for protons and helium nuclei are 100%, and reconstruction efficiencies for protons and helium nuclei are 99% and 97%, respectively. The background contribution for protons and helium nuclei are 4% and 5%.

The live time T is 23 days. Excluding data collected during tuning periods for the first few days, the live time versus total time is 99%. The attenuation loss in the atmosphere (3.9 g/cm^2) and material depth of detector (12 g/cm^2) above the SCD are about 79% for protons and 65% for helium nuclei.

Secondaries due to interactions with material above the SCD are about 16% for protons and 24% for helium

nuclei. The effects of secondary production will be estimated more accurately with MC simulation information using the CREAM-III detector configuration in the near future.

In this analysis, the efficiencies and background were calculated independently of energy constant since the thresholds were set as low as 1 TeV. Energy-dependent efficiency calculations near thresholds might extend the data to lower energies when the MC simulation event sets for lower energy are ready.

IV. RESULTS

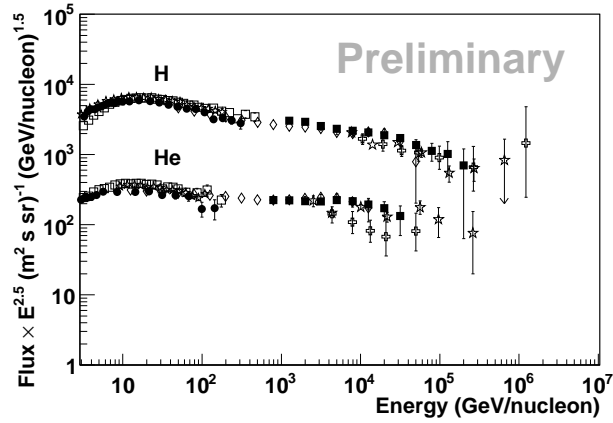
The CREAM-III preliminary proton flux at the top of the atmosphere from 1 TeV to 250 TeV and helium flux from 400 GeV/n to 4 TeV/n are shown in Fig. 2a. Also shown are previous measurements from AMS [16],[17], BESS-TeV [18], CAPRICE98 [19], ATIC-2 [20], JACEE [21], and RUNJOB [22]. The preliminary CREAM-III proton and helium spectra are consistent with a power law, within statistical uncertainties. The CREAM-III proton spectrum is in good agreement with recent ATIC-2, RUNJOB, and JACEE results. The CREAM-III helium flux agrees with ATIC-2 and JACEE results. The helium spectrum appears flatter than the proton spectrum in CREAM-III.

The preliminary proton to helium ratio from CREAM-III is shown in Fig. 2b together with previous measurements from BESS-TeV [18], CAPRICE94 [23], CAPRICE98 [19], ATIC-2 [20], LEAP [24], JACEE [25], and RUNJOB [26]. The CREAM-III ratio extends the ATIC-2 results to higher energy and shows good agreements with recent ATIC-2 and JACEE results. The CREAM-III ratios show lower values than previous low-energy measurements below 100 GeV/n, such as BESS, CAPRICE94, CAPRICE98, and LEAP. This is consistent with the higher helium flux of CREAM-III than was measured at lower energies for helium. Above 10 TeV, statistics grow sparse, so more data are necessary.

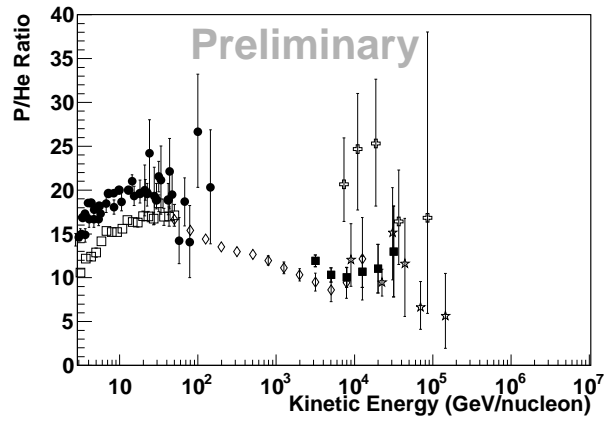
V. SUMMARY

The measured proton and helium spectra during the CREAM-III flight are being measured. Preliminary results are shown in comparison with previous measurements. During the CREAM-III flight, more data were collected at lower energies than during the CREAM-I flight, as expected from the lower thresholds. The preliminary CREAM-III proton and helium spectra are in good agreement with previous measurements within the uncertainties. More MC simulations with the CREAM-III flight configuration are in progress. The energy deconvolution and efficiency calculation will be improved with more MC simulation results. Also, analysis using both the top and bottom SCDs in charge identification will improve the results.

Acknowledgment



(a) Preliminary CREAM-III proton and helium spectra



(b) Proton to helium ratio

Fig. 2. Preliminary CREAM-III (filled square) proton and helium fluxes (rescaled by $E^{2.5}$) are shown together in Fig 2a with previous experiments; AMS (open star), BESS-TeV (open square), CAPRICE98 (open inverse triangle), ATIC-2 (open diamond), JACEE (open star) and RUNJOB (open cross). For CREAM-III, statistical uncertainties are shown. Preliminary CREAM-III proton to helium ratios are shown in Fig. 2b together with previous measurements; ATIC-2, BESS-TeV, CAPRICE94 (diamond with cross), CAPRICE98, JACEE, LEAP (circle with cross), and RUNJOB (symbols as for Fig. 2a).

The authors thank NASA Wallops Flight Facility, Columbia Scientific Balloon Facility, National Science Foundation Office of Polar Programs, and Raytheon Polar Service Company for the successful balloon launch, flight operations, and payload recovery. This work is supported by NASA in the U.S., KICOS and Ministry of Science and Technology in Korea, and IN2P3, CNRS, and CNES in France.

REFERENCES

- [1] Asakimori, K. *et al.* 1998, ApJ, 502, 278
- [2] Apanasenko, A.V. *et al.* 2001, Astropart. Phys., 16, 13
- [3] Seo, E.-S. *et al.* 2004, Adv. Spa. Res., 33, 1777
- [4] Seo, E.-S. *et al.* 2009, J. Phys. Soc. Jpn., 78, 63
- [5] Ahn, H.S. *et al.* 2007, Nucl. Instrum. Methods A, 581, 133
- [6] Park, I.H. *et al.* 2007, Nucl. Instrum. Methods A, 570, 286
- [7] Ahn, H.S. *et al.* 2009, Nucl. Instrum. Methods A, 602, 525
- [8] Y. Sallaz-Damaz *et al.* 2008, Nucl. Instrum. Methods A, 595, 62
- [9] Lee, M.H. *et al.*, IEEE Tran. on Nucl. Sci., accepted for publication, Dec. 2008
- [10] Han, J.H. *et al.*, "Performance in flight of the CREAM-III and CREAM-IV calorimeter", in this conference
- [11] Park, N.H. *et al.* 2007, Nucl. Instrum. Methods A, 581, 133
- [12] Burn, R.F. *et al.* GEANT User Guide, CERN DD/EE/84-1, Geneva, 1984
- [13] Fasso, A. *et al.* Proc. IV Int. Conf. on Calorimetry in High Energy Physics, La Biodola, Italy, 21-26 Sept. 1993, Ed A. Menzione and A. Scribano, World Scientific, p. 493
- [14] Han, J.H. *et al.*, "Calibration of the CREAM-III calorimeter with beam test data", in this conference
- [15] Ahn, H.S. *et al.* 2006, Adv. Spa. Res., 37, 1950
- [16] Alcazar, J. *et al.* 2000, Phys. Lett. B, 490, 27
- [17] Alcazar, J. *et al.* 2000, Phys. Lett. B, 494, 93
- [18] Haino, S. *et al.* 2004, Phys. Lett. B, 594, 35
- [19] Boezio, M. *et al.* 2003, Astropart. Phys., 19, 583
- [20] Wefel, J.P. *et al.* 2007, Proc. 30th Int. Cosmic-Ray Conf.(Merida), 2, 31
- [21] Asakimori, K. *et al.* 1998, ApJ, 502, 278
- [22] Apanasenko, A.V. *et al.* 2001, Astropart. Phys., 16, 13
- [23] Boezio, M. *et al.* 1999, ApJ, 518, 457
- [24] Seo, E.S. *et al.* 1991, ApJ, 378, 763
- [25] Asakimori, K. *et al.* 1993, Proc. 23rd Int. Cosmic-Ray Conf.(Calgary), 2, 25
- [26] Hareyama, M. and Shibata, T. for RUNJOB collaboration 2006, J. of Phys.:Conf. Ser., 47, 106